INDIVIDUAL VARIATION IN DISPERSAL AND FECUNDITY INCREASES RATES OF SPATIAL SPREAD

SEBASTIAN J. SCHREIBER AND NOELLE G. BECKMAN

Abstract. Dispersal and fecundity are two fundamental traits underlying the spread of populations. Using integral difference equation models, we examine how individual variation in these fundamental traits and the heritability of these traits influence rates of spatial spread of populations along a one-dimensional transect. Using a mixture of analytic and numerical methods, we show that individual variation in dispersal rates increases spread rates and the more heritable this variation, the greater the increase. In contrast, individual variation in lifetime fecundity only increases spread rates when some of this variation is heritable. The highest increases in spread rates occurs when variation in dispersal positively covaries with fecundity. Our results highlight the importance of estimating individual variation in dispersal rates, dispersal syndromes in which fecundity and dispersal co-vary positively, and heritability of these traits to predict population rates of spatial spread.

Predicting population dynamics over space and time is a central question in ecology and critical for understanding how species will respond to global change [Hastings et al., 2005, Jongejans et al., 2008]. Incorporating demography and dispersal with theoretical models to understand and predict the spatial spread of populations over time has a long history [Fisher, 1937, Skellam, 1951], and new mathematical insights in the ecology and evolution of spatial spread are continuing to emerge [Hastings et al., 2005, Beckman et al., in press]. Spatial demographic models have been used to aid in conservation and management decisions to control the spread of invasive species [e.g., Shea et al., 2010] and to predict the persistence of species under shifting climates [e.g., Santini et al., 2016, Travis et al., 2011]. These models typically rely on mean estimates of dispersal parameters and demographic responses [but see Jongejans et al., 2011], however these can vary across individuals within populations [reviewed in Schupp et al., in revision], with important consequences for population, communities, and evolution [Bolnick et al., 2011, Moran et al., 2016, Snell et al., 2019].

Populations can respond to global change by tracking their ecological niche through space [e.g., Tingley et al., 2009] or adapting to the new environmental conditions [Hoffmann and Sgro, 2011]. Traits have been shown to respond rapidly to environmental change due to plasticity or rapid evolution [Ellner, 2013, Johnson et al., 2019]. Theoretical studies suggest the evolution of increased dispersal [Travis and Dytham, 2002, Phillips et al., 2008, Hughes et al., 2007], increased reproduction [Burton et al., 2010], and traits related to competition (decreased competitive ability, Burton et al. 2010; increased competitive tolerance, Williams et al. 2016b) on the edges of a species' expanding range [Phillips et al., 2010]. Moreover, models show that these evolutionary changes can result in accelerating spread [Bouin et al., 2012, Phillips et al., 2008, Perkins et al., 2013, Travis et al., 2009]. Empirical studies of expanding plant populations have supported some of these theoretical predictions [Cwynar and MacDonald, 1987, Huang et al., 2015, Williams et al., 2016a, Tabassum and Leishman, 2018, 2019]. While there is increasing consideration for the evolution of dispersal

or life history traits affecting spread rates of populations, we lack a full understanding of how variation in dispersal, variation in life history traits, and their covariation may facilitate or constrain population spread rates.

Dispersal and life history traits may covary to produce integrated strategies known as dispersal syndromes [Ronce and Clobert, 2012] or dispersal may vary independently from other life history traits [Bonte and Dahirel, 2017]. Across species, Beckman et al. [2018] found evidence for plant dispersal syndromes. Species with fast life-history strategies dispersed their seeds further than species with slow life-history strategies, potentially as a bet-hedging strategy. Specifically, species with high dispersal ability also had high net reproductive rate, a long window of reproduction, low likelihood of escaping senescence, and low shrinkage [Beckman et al., 2018]. Within species, dispersal is predicted to be an independent axis of other life history traits [Bonte and Dahirel, 2017], although this is not well-studied in plants. Whether and how dispersal and life history traits co-vary influence the ability of organisms to evolve in response to environmental change.

In plants, variation in dispersal arises from intrinsic variation in trait expression among and within individuals and extrinsic variation based on the environmental context of the plant [Schupp et al., in revision, Saastamoinen et al., 2018]. Saastamoinen et al. [2018] found that while plants can have have high levels of heritability in dispersal traits, there can be a wide range of heritability that depends on the specific trait measured and the environment in which it was measured. Evolutionary change in dispersal also depends on the covariance of dispersal with other traits under selection [Saastamoinen et al., 2018]. Within populations, higher fecundity in plants is expected to increase the distance seeds are dispersed [Clark et al., 1998a, Norghauer et al., 2011]. The number of fruit produced varies substantially among individuals within and across years in natural systems [e.g., Norghauer et al., 2011, Norghauer and Newbery, 2015] with moderate to high heritability found in crop systems [e.g., Jindal et al., 2010, Usman et al., 2014].

Most predictive models of population spread tend to ignore trait variability, and fewer have examined hertiable trait variation [Johnson et al., 2019]. Incorporating trait evolution into demographic models will increase our understanding and prediction of population responses to environmental change [Urban et al., 2016] that can help inform management and conservation. Previous studies have shown that rates of spatial spread increase with either non-heritable variation in disperal rates creating leptokeurtic dispersal kernels [Petrovskii and Morozov, 2008, Stover et al., 2014] or heritable variation selecting for higher dispersal rates [Bouin et al., 2012, Phillips et al., 2008, Perkins et al., 2013, Travis et al., 2009]. However, the simultaneous effects of heritable and non-hertible co-variation in dispersal and demographic rates on spatial spread remains to be understood. Here, we tackle this issue using integral difference equation models of spatial spread accounting for fecundity and dispersal variation that is either perfectly or randomly transmitted due to modifier genes regulating transmission of these traits [Altenberg et al., 2017].

Model and Methods

Our models consider a population of plants living along a one-dimensional transect. Individuals vary in their production of seeds and the mean distance that a seed disperses. We consider two forms of the model: one with random transmission of individual traits and another allowing for non-random transmission of the traits. Both forms of the models are integro-difference equations that have been used extensively to model spatial spread [Kot

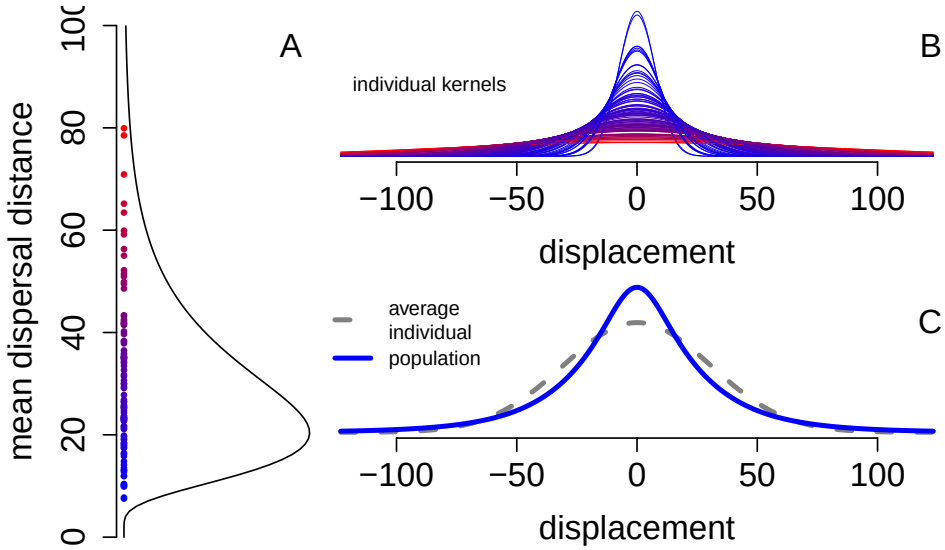

FIGURE 1. Individual variation in dispersal rates and the population-level dispersal kernel. In (A), variation among 100 maternal trees in their seed dispersal rates (mean dispersal distance). In (B), the Gaussian dispersal kernels of the 100 individuals from (A). In (C), the population-level dispersal kernel (i.e. the average of the kernels from (A)) in solid blue and the dispersal kernel of individuals with the average dispersal rate in dashed gray.

et al., 1996, Neubert and Caswell, 2000]. For the model with non-random transmission, the population is structured by the trait in every spatial location. The changes in this local population structure are determined by a matrix model for discretely-structured traits and by an integral projection model for continuously-structured traits. For both types of models, we use the methods of Ellner and Schreiber [2012] to identify the asymptotic rates of spatial spread. Using these methods, we develop explicit formulas for both forms of individual variation to examine how they alter spatial rates of spread. As these formulas are derived in the limit of small individual variation, we also numerically analyze an empirically-based model to illustrate how the insights from our formulas are also applicable when individual variation is larger.

Models with random transmission. Let $n_t(x)$ denote the population density at location x in generation t. Under low-density conditions, individual plants produce f seeds during their life time. Each of these seeds disperse, on average, a distance of ℓ meters. We call this mean dispersal distance, the dispersal rate i.e. the average number of meters a seed moves in a generation. The density of individuals within the population with these characteristics of fecundity and dispersal equal $\rho(f,\ell)$. For seeds with a dispersal rate of 1 meter, let $k_1(v)dv$ be the infinitesimal probability that these seeds disperse from location x to location $x+v$. Then, the dispersal kernel for a group of seeds with dispersal rate ℓ equals $k_\ell(v) = k_1(v/\ell)/\ell$. The density of individuals with disperal rate ℓ is given by the marginal density $\rho_L(\ell) = \int \rho(f,\ell)\,df$. The population-level dispersal kernel corresponds to averaging dispersal kernels k_ℓ across this individual variation (Fig. 1):

$$k_{\text{pop}}(v) = \int k_\ell(v)\rho_L(\ell)d\ell.$$

Petrovskii and Morozov [2008] call this population-level kernel a statistically structured dispersal model.

If $D(n_t(y))$ corresponds to a density-dependent reduction in life-time fecundity at location y, then the spatial dynamics of the population is

$$n_{t+1}(x) = \int_{-\infty}^{\infty} \left(\iint k_\ell(x-y) f \rho(f,\ell) d\ell df \right) D(n_t(y)) n_t(y) dy. \tag{1}$$

Without loss of generality, we assume that $D(0) = 1$. Furthermore, we assume that $D(n) \leq D(0)$ for all densities $n \geq 0$ i.e. the lifetime fecundity of an individual is maximal at low densities. This assumption allows us to use the linearization principle for computing invasion speeds [Kot et al., 1996, Neubert and Caswell, 2000, Ellner and Schreiber, 2012].

While we have presented our model in equation (1) for continuously-structured traits, one can write a similar model for discretely-structured traits by replacing the double integral $\iint$ with a double sum $\sum_i \sum_j$ and replacing the infinitesimal probabilities $\rho(f,\ell)df d\ell$ with discrete probabilities $\rho(f_i,\ell_j)$ for each of the traits. For example, the population-level dispersal kernel for discretely-structured population variation is $\sum_j k_{\ell_j}(v)\rho_L(\ell_j)$ where $\rho_L(\ell_j) = \sum_i \rho(f_i,\ell_j)$ is the marginal distribution of the individual dispersal rates (Fig. 1).

Accounting for perfect transmission of traits. Following Altenberg et al. [2017], we consider a model where there is a mixture of random transmission and perfect inheritance. Due to seeds potentially inheriting their traits from their parents, this model needs to keep track of the density of individuals of a given trait combination at a given location. Let $n_t(x; f, \ell)$ be the density of individuals of type f, ℓ at location x at time t. Let ν be the probability of perfect inheritance. When the trait isn't perfectly transmitted, it is randomly transmitted with respect to the density $\rho(f,\ell)$; this allows to compare models with and without heritability. One mechanism that can lead to this form of inheritance are modifier genes [Altenberg et al., 2017].

Under these assumptions, the model with perfect transmission is

$$\begin{aligned} n_{t+1}(x; f, \ell) = \int_{-\infty}^{\infty} k_\ell(x-y) \times D\left(\iint n_t(y, f', \ell') df' d\ell' \right) \times \\ \left(\nu f n_t(y; f, \ell) + (1-\nu)\rho(f,\ell) \iint f' n_t(y; f', \ell') df' d\ell' \right) dy \end{aligned} \tag{2}$$

where $D\left(\iint n_t(y, f', \ell') df' d\ell'\right)$ is the density-dependent reduction in fecundity at location y due to the total population density $\iint n_t(y, f', \ell') df' d\ell'$ at location y. For discretely-structured traits, we can use the same model structure by replacing the double integrals $\iint df d\ell$ and $\iint df' d\ell'$ with a double sums $\sum_i \sum_j$ that sum over all the traits, and replacing the infinitesimal probabilities $\rho(f,\ell)df d\ell$ with discrete probabilities $\rho(f_i,\ell_j)$ for each of the traits.

Analytic methods. To compute the asymptotic rates of spatial spread in both models, we make use of the linearization conjecture [Kot et al., 1996, Neubert and Caswell, 2000, Ellner and Schreiber, 2012] whose assumptions are satisfied whenever the base dispersal kernel $k_1(v)$ has exponentially bounded tails and the density $\rho(f,\ell)$ is compactly supported i.e. there exist $f_{\min} < f_{\max}$ and $\ell_{\min} < \ell_{\max}$ such that $\iint \rho(f,\ell) df d\ell = \int_{f_{\min}}^{f_{\max}} \int_{\ell_{\min}}^{\ell_{\max}} \rho(f,\ell)\, df\, d\ell = 1$.

To use the linearization conjecture for the model with random transmission, we use the transform

$$\lambda(s) = \int_{-\infty}^{\infty} \iint f e^{sv} \frac{k_1(v/\ell)}{\ell} \rho(f,\ell) df d\ell dv$$

for the combined demography and dispersal kernel at low density. The linearization conjecture asserts that the asymptotic rate of spatial spread equals

$$c^* = \min_{s>0} \frac{\log \lambda(s)}{s} \tag{3}$$

where the minimum is taken over values of s for which $\lambda(s)$ is well-defined. For the model with perfect transmission, define the full demography and dispersal kernel $K(f,\ell;f',\ell',v)$ by

$$K(f,\ell;f',\ell',v) = k_\ell(v)\left(\nu f \delta_{(f,\ell)}(f',\ell') + (1-\nu) f \rho(f',\ell')\right)$$

where $\delta_{(f,\ell)}(f',\ell')$ is the Dirac delta function at (f,ℓ). Let $H(s)$ be the operator that takes function of the form $n(f,\ell)$ to the function

$$(Hn)(f',\ell') = \int_{-\infty}^{\infty} \left(\iint K(f,\ell;f',\ell',v) e^{sv} df d\ell \right) dv$$

and let $\lambda(s)$ be the dominant eigenvalue of $H(s)$. Then the asymptotic rate of spatial spread is, once again, given by equation (3). When the individual variation is discretely structured, these formulas still apply but the double integrals $\iint$ need to be replaced with double sums $\sum_i \sum_j$ and the density functions need to be replaced with probability distribution functions as described in the model section.

We use equation (3) in three ways. First, we approximate its solution for small variances. Namely, let F and L be random variables with joint density $\rho(f,\ell)$. Then we can express these random variables in the form $F = \overline{F} + \sigma_F^2 Z_F$ and $L = \overline{L} + \sigma_L^2 Z_L$ where $\overline{F}$, σ_F^2 are the mean and variance of the fecundity, $\overline{L}$, σ_L^2 are the mean and variance of the mean dispersal distance L, and $Z_F = (F - \overline{F})/\sigma_F, Z_L = (L - \overline{L})/\sigma_L$ are random variables with a mean of 0 and variance of 1. In Appendix A, we derive approximations for the rates of spatial spread when σ_F^2 and σ_L^2 are sufficiently small. Second, to understand the effect of perfect transmission on rates of spatial spread, we use the reduction principle [Altenberg and Feldman, 1987, Liberman and Feldman, 1986, Altenberg, 2012] to show that the rate of spatial spread increases with the probability ν of perfect transmission. Moreover, we derive an explicit approximation of the rate of spread for low levels of perfect transmission in Appendix B.

Finally, we use equation (3) for our numerical calculations. The numerical calculations were based on empirical fits of dispersal data for the tree *Acer rubrum* [Clark et al., 1998b, Clark, 1998]. Clark et al. [1998b] collected data on seed rain over 5 years from 100 seed traps located within five 0.36-ha mapped tree stands in the southern Appalachians. When fit with a Gaussian dispersal kernel, the distance parameter α equals $30.8 \pm 3.80SE$ (average distance traveled is $\alpha\Gamma(1)/\Gamma(1/2) = 17.4$). Clark [1998] estimated the net reproductive rate as $1,325$ and the generation time at $T = 5.8$ years. To get yearly rates of spread, we followed Clark [1998] and used c/T.

Results

Let $\overline{F}$ and $\overline{L}$ be the mean lifetime fecundity and mean dispersal rate of the population: $\overline{F} = \iint f\rho(f,\ell) df d\ell$ and $\overline{L} = \iint \ell\rho(f,\ell) df d\ell$. Let σ_F^2 and σ_L^2 be the associated variances:

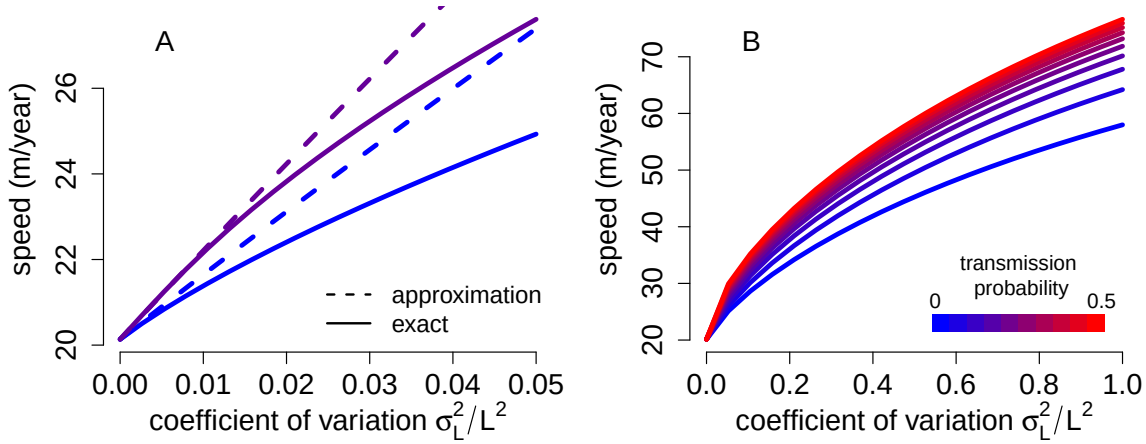

FIGURE 2. Individual variation in dispersal rates increases rate of spatial spread. Rates of spatial spread for *Acer rubrum* (see *Methods*) are plotted against the coefficient of variation of the dispersal rate and for increasing probabilities of perfect transmission (from blue to red). For low variability and transmission probabilities, the analytical approximations (dashed lines in panel A) provide a good approximation to the exact invasion speeds (solid lines). Higher levels of variation (panel B) have a decelerating effect on rates of spatial spread.

$\sigma_F^2 = \iint (f-\overline{F})^2 \rho(f,\ell) df d\ell$ and $\sigma_L^2 = \iint (\ell-\overline{L})^2 \rho(f,\ell) df d\ell$. Let r be the correlation between the lifetime fecundity of individuals and the dispersal rates of their seeds: $r = \iint (f-\overline{F})(\ell-\overline{L})\rho(f,\ell) df d\ell/(\sigma_F \sigma_L)$. Let $m(s) = \int_{-\infty}^{\infty} k_1(v/\overline{L})/\overline{L}\, dv$ be the moment generating function for the dispersal kernel of the mean dispersal phenotype.

Individual variation in dispersal rates. Using analytical approximations for small individual variation in dispersal rates, Appendix A demonstrates that randomly transmitted variation in dispersal rates increases the rate of spatial spread by a term proportional to the squared coefficient of variation in the mean dispersal distances. Specifically, for sufficiently small variance σ_L, the increase is the spread rate equals

$$\frac{m''(s^*)s^*}{2m(s^*)} \times \left(\frac{\sigma_L}{\overline{L}}\right)^2. \tag{4}$$

The proportionality constant $\frac{m''(s^*)s^*}{2m(s^*)}$ is proportional to the variance in the dispersal distances traveled by individuals with a mean dispersal distance of $\overline{L}$; the greater this variance, the greater the increase in the rate of spread. Intuitively, if the base mode of dispersal has greater variation in distances traveled (e.g. the Laplacian kernel with a fatter tail versus the normal with a thinner tail), the greater the likelihood of individuals moving greater distances and it is these individuals that determine the rate of spatial spread.

When some of the variation in mean dispersal distances is perfectly transmitted to offspring, the reduction principle [Altenberg and Feldman, 1987, Liberman and Feldman, 1986, Altenberg, 2012] implies there is an additional increase in the rate of spread. When the variation in dispersal rates is small and the probability of perfect transmission is small, Appendix

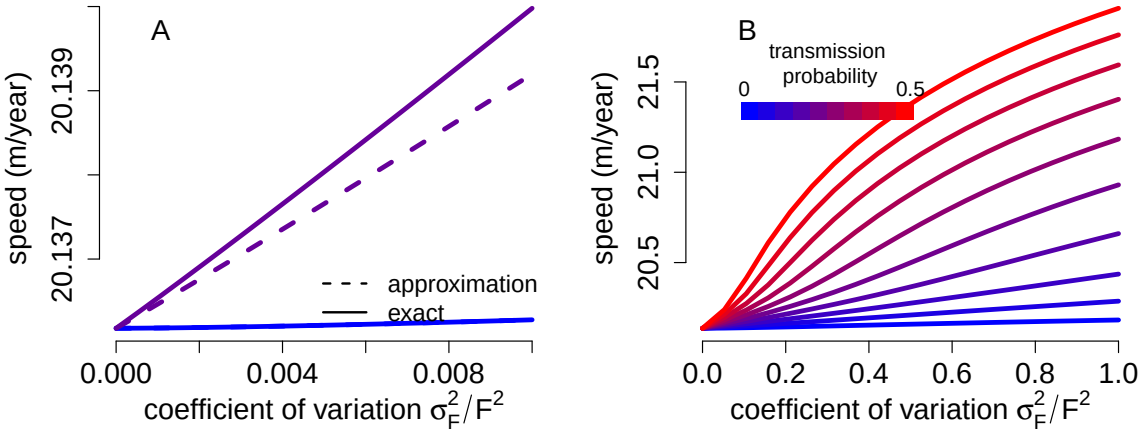

FIGURE 3. Individual variation in fecundity increases rate of spatial spread only when it is heritable. Invasion speeds for *Acer rubrum* (see *Methods*) are plotted against the coefficient of variation of fecundity and for increasing probabilities of perfect transmission (from blue to red). For low variability and transmission probabilities, the analytical approximations (dashed lines in panel A) provide a good approximation to the exact invasion speeds (solid lines). Higher levels of variation (panel B) have nonlinear effects on these invasion speeds.

B demonstrates that this additional increase is proportional to the product of the coefficient of variation in the mean dispersal distance and the probability of perfect transmission. Specifically,

$$\frac{m'(s^*)^2 s^*}{m(s^*)^2} \times \left(\frac{\sigma_L}{\overline{L}}\right)^2 \times \nu. \tag{5}$$

Numerical calculations for *Acer rubrum* based on equation (3) show that the linear trend predicted by analytical approximation holds at low levels of variation (Figure 2A) but break down at higher levels of variation (Figure 2B). The effect of individual variation in dispersal rates on rates of spatial spreads saturates with increasing levels of variation. None the less, the qualitative trends of variation in dispersal rates and perfect transmission of this variation increasing rates of spread still hold. Notably, even for moderate levels of variation and perfect transmission, individual variation in dispersal rates give substantial boosts to the predicted rate of spread for *Acer rubrum*. For example, a squared coefficient of variation of 0.5 more than doubles the rate of spatial spread (from approximately 20m/year to approximately 45m/year). If half of this variation is perfectly transmitted, then the spread rate nearly triples to 60m/year.

Individual variation in fecundity. Randomly transmitted variation in fecundity has no effect on rates of spatial spread. However, when some of this variation is perfectly transmitted, the reduction principle implies there is an increase in the spread rate. For low levels of individual variation in fecundity and perfect transmission, Appendix B demonstrates that the invasion speed increases by a term proportional to the product of the squared coefficient of variation

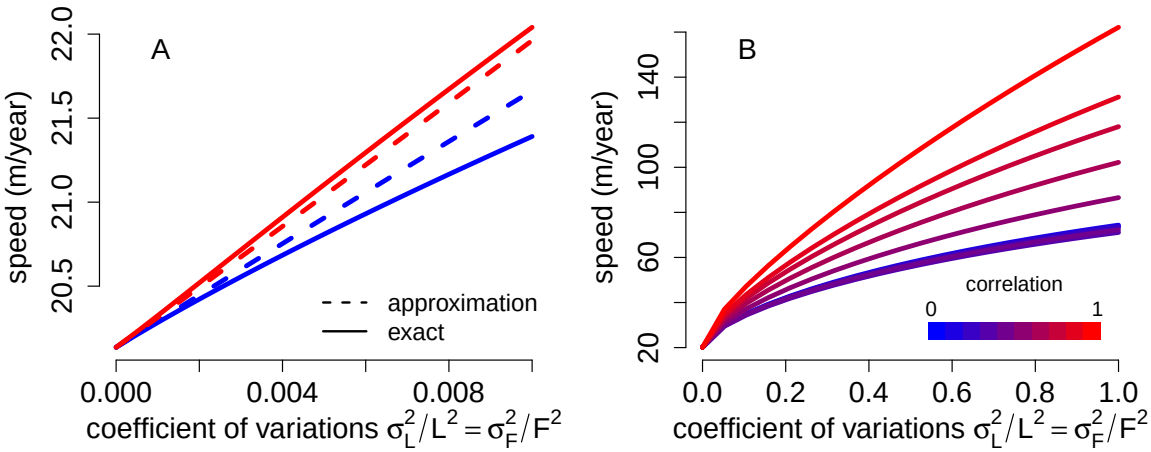

FIGURE 4. Covariation in fecundity and dispersal rates leads to faster rates of spatial spread. Invasion speeds for *Acer rubrum* (see *Methods*) are plotted against the coefficient of variations of fecundity and dispersal rates, and for increasing correlations between fecundity and dispersal rates (from blue to red). For low variability, the analytical approximations (dashed lines in panel A) provide a good approximation to the exact invasion speeds (solid lines). Higher levels of variation (panel B) have a nonlinear effect on invasion speeds. Probability of perfect transmission is 0.1 in (A) and is 0.5 in (B).

in fecundity and the probability of perfect transmission. Specifically,

$$\frac{1}{s^*} \times \left(\frac{\sigma_F}{\overline{F}}\right)^2 \times \nu. \tag{6}$$

Figure 3 illustrates these effects numerically using equation (3) for the *Acer rubrum* model. In contrast to individual variation in dispersal rates, heritable variation in fecundity has small effects on rates of spatial spread. For example, a coefficient of variation of 1 with a 50% chance of perfect transmission, speeds only increase approximately 9% for fecundity variation (Fig. 3B) in contrast to approximately 380% for dispersal variation (Fig. 2B). This relative small increase in the rate of spatial spread stems from the relatively small proportionality constant $1/s^* \approx 8$ in (6) compared to the proportionality constants in equation (4) with $\frac{m''(s^*)s^*}{2m(s^*)} \approx 900$ and equation (5) with $\frac{m'(s^*)^2 s^*}{m(s^*)^2} \approx 1700$.

Covariation in dispersal rates and fecundity. If lifetime fecundity of parents covary with dispersal rates of their seeds and this variation is randomly transmitted, then we show analytically in Appendix A that the spread rate increases by two terms: the amount due to dispersal variation alone in equation (4) plus an additional term proportional to the covariance of L and F:

$$\frac{m'(s^*)}{m(s)} \times r \times \frac{\sigma_L}{\overline{L}} \times \frac{\sigma_F}{\overline{F}}. \tag{7}$$

If this covariation is perfectly transmitted with probability ν, then the reduction principle implies that there is another additional increase to the spread rate. For low levels of individual variation and perfect transmission, Appendix B shows this additional increase is

proportional to the product of the covariance between fecundities and dispersal rates and the probability of perfect transmission:

$$\frac{2m'(s^*)}{m(s^*)} \times r \times \frac{\sigma_L}{\overline{L}} \times \frac{\sigma_F}{\overline{F}} \times \nu. \tag{8}$$

For the *Acer rubrum* model, Figure 4 illustrates the substantial increase due to this covariation: high positive correlation and heritability of individual variation in fecundity and dispersal rates (red curve in Fig. 4B) can lead to an eight-fold increase in the rate of spatial spread (approximately 160m/year) compared to the less than four fold increase (approximately 74m/year) due to uncorrelated variation in fecundity and dispersal rates (blue curve in Fig. 4B).

Discussion

Dispersal and fecundity are two fundamental traits underlying the spread of populations [Fisher, 1937, Skellam, 1951, Kot et al., 1996, Neubert and Caswell, 2000]. We show that inclusion of individual variation and covariation of these traits shifts predictions of population spread. Our results indicate that variation in dispersal increases spread rates of populations regardless of the mode of transmission, while variation in fecundity only increases spread rates when some of this variation is heritable. The highest increases in spread rates occurs when variation in dispersal positively covaries with fecundity. Spread rates generally increase as the probability of perfect transmission in variation in dispersal, variation in fecundity, or covariation in dispersal and fecundity increase. Although we focus on plants, our results are also applicable to animal systems

Our results are in-line with previous mathematical studies that show accelerated spread rates when individuals within the population vary in their dispersal ability [Bouin et al., 2012, Stover et al., 2014]. For gamma-distributed variation in dispersal rates and uniform distributions on two dispersal rates, Stover et al. [2014] showed that the moment generating functions of the population-level dispersal kernels increase with individual variation in dispersal rates and, thereby, increase spread rates. However, their numerical explorations found modest increases in spread rates when compared to our *Acer rubrum* example (e.g. about 20% in [Stover et al., 2014, Fig.3] versus 300% increase in spread rates for a squared coefficient of variation of 1). Our analytic approximation (see equation (4)) implies that this difference stems from the estimated mean dispersal rate of *Acer rubrum* being greater than the base dispersal rate used by Stover et al. [2014] (i.e. 30.8m/year versus 1m/year) which produces larger differences in the proportionality constant of equation (4). When intraspecific variability in dispersal rates is mostly heritable (i.e. mutation rates are low), Bouin et al. [2012] demonstrated that the spread rate is essentially determined by the genotypes with the highest dispersal rate being selected for at the edge of the spatial range i.e. spatial sorting. Complementing this result, we show that, care of Karlin's reduction principle [Altenberg, 2012, Altenberg et al., 2017], lower levels of heritability lead to progressively smaller increases in spread rates. Indeed, at low levels of heritability (see equation (5)), the increase in spread rates is constrained by the coefficient of variation in the dispersal rates and the shape of population's base dispersal kernel.

In contrast to individual variation in dispersal rates, we find that non-heritable variation in fecundity has no effect on rates of spatial spread. This outcome stems from (i) our analysis focusing on populations being sufficiently large that demographic stochasticity is negligible

and (ii) the Laplace transform of the demography-dispersal kernel being a linear function of local demographic rates and a convex function of dispersal rates. As local demographic stochasticity slightly decreases spread rates [Snyder, 2003, Reluga, 2016] and individual variation in fecundity increases demographic stochasticity [Lloyd-Smith et al., 2005], it seems likely that demographic stochasticity coupled with individual variation in fecundity would decrease spread rates further. In contrast, we found that heritable variation in fecundity increases rates of spatial spread. In the extreme of this variation being perfectly transmitted from parents to offspring, we anticipate that spread rates are determined by selection for the most fecund individuals throughout the spatial range, unlike the spatial sorting mechanism found by Bouin et al. [2012] for heritable variation in dispersal rates.

We find the biggest effects of individual variation when dispersal rates and fecundity covary to form dispersal syndromes within species. Specifically, positive covariation of these traits, as has been found for some wind- and endozoochorous-dispersed seeds [reviewed in Schupp et al., in revision, Snell et al., 2019], always increases spread rates (e.g., more than doubling spread rates for *Acer rubrum*). Heritability of this covariation leads to greater increases of spatial spread. For example, our analysis implies that 50% heritability of this covariation can double the increase in spread rates (i.e. equations (7) and (8) are equal when $\nu = 0.5$). In contrast, we found that negative correlations between fecundity and dispersal rates lead to slower spread rates, but these rates are still higher than if there were no individual variation in fecundity or dispersal. Interestingly, Elliott and Cornell [2012] demonstrated that when there is trade-off between fecundity and dispersal (i.e. a negative correlation), polymorphisms of high and low fecundity individuals maintained by mutation would lead to higher spread rates than the monomorphic spread rates. It would be interesting to know whether such mechanisms are operating in natural systems and whether such polymorphisms can lead to faster spread rates than monomorphic populations without tradeoffs between fecundity and dispersal.

Here we consider the influence of variation in dispersal, variation in fecundity, and their covariation on population spread rates assuming the environment is spatially homogeneous. However, spatially heterogeneous environments may alter these predictions. Heterogeneous environments can arise from natural disturbances, such as tree fall gaps, or through habitat loss and destruction due to human impacts. The latter is one of the leading causes of biodiversity loss [Pereira et al., 2010] and tends to result in the fragmentation of the landscape into smaller, isolated fragments within a human-modified matrix. Fragmentation can alter the evolution of population expansion such that competitive tolerance (i.e., maintaining high fecundity at high density) is favored at the invading front [Williams et al., 2016b]. Consistent with these theoretical results, evolving populations of *Arabidopsis thaliana* in experimental landscapes spread much faster in fragmented than continuous landscapes due to the selection for dispersal and competitive tolerance [Williams et al., 2016a]. However, a high cost of dispersing to low quality habitat in a fragmented landscape can result in rapid evolution of reduced dispersal [Travis and Dytham, 2002], as was shown for the herb *Crepis sancta* in response to recent colonization of an urban landscape [Cheptou et al., 2008]. The process of fragmentation is expected to influence the diversity of dispersal syndromes that evolve across the landscape [Cote et al., 2017]. For example, in highly variable fragments surrounded by an unsuitable matrix, non-dispersing individuals may have life history and phenotypic traits more suitable to surviving and growing in the same fragment as the source tree versus dispersing individuals may have traits more suitable to move across an inhospitable matrix

and survive and grow in another fragment with differing conditions [Cote et al., 2017]. A challenge for future work is understanding how both heritable and non-heritable individual variation trait interacts with this spatial variation to determine rates of spatial spread.

Conclusion. Predictions of spread tend to rely on mean estimates of population parameters for dispersal and life history traits, but these may vary within a population and evolve through time. We found increased heritability in dispersal and fecundity increases spread rates compared to random transmission of traits, and if these are positively covarying to form dispersal syndromes within species, selection further facilitates increased spread rates. However, if dispersal and fecundity co-vary with other life history traits, selection for these traits may be constrained by or indirectly influence the evolution of other life-history traits, such as competitive ability or defense against natural enemies. The degree to which plant populations exhibit heritability of variation in dispersal or dispersal syndromes in which fecundity and dispersal co-vary positively is key to predicting the speed at which populations will track shifting habitats.

References

L. Altenberg. Resolvent positive linear operators exhibit the reduction phenomenon. *Proceedings of the National Academy of Sciences*, 109:3705–3710, 2012.

L. Altenberg and M.W. Feldman. Selection, generalized transmission and the evolution of modifier genes. i. the reduction principle. *Genetics*, 117:559–572, 1987.

L. Altenberg, U. Liberman, and M.W. Feldman. Unified reduction principle for the evolution of mutation, migration, and recombination. *Proceedings of the National Academy of Sciences*, 114:E2392–E2400, 2017.

N. G. Beckman, J. M. Bullock, and R. Salguero-Gómez. High dispersal ability is related to fast life history strategies. *Journal of Ecology*, 106:1349–1362, 2018.

N. G. Beckman, C. E. Aslan, H. S. Rogers, O. Kogan, J. L. Bronstein, J. M. Bullock, F. Hartig, J. HilleRisLambers, Y. Zhou, D. Zurell, J. F. Brodie, E. M. Bruna, R. S. Cantrell, R. R. Decker, E. Effiom, E. C. Fricke, K. Gurski, A. Hastings, J. S. Johnson, B. A. Loiselle, M. N. Miriti, M. G. Neubert, L. Pejchar, J. R. Poulsen, G. Pufal, O. H. Razafindratsima, M. E. Sandor, K. Shea, S. Schreiber, E. W. Schupp, R. S. Snell, C. Strickland, and J. Zambrano. Advancing an interdisciplinary framework to study seed dispersal ecology. *AoB Plants*, in press.

D. I. Bolnick, P. Amarasekare, M. S. Araújo, R. Bürger, J. M. Levine, M. Novak, V.H.W. Rudolf, S.J. Schreiber, M.C. Urban, and D.A. Vasseur. Why intraspecific trait variation matters in community ecology. *Trends in Ecology & Evolution*, 26:183 – 192, 2011.

D. Bonte and M. Dahirel. Dispersal: a central and independent trait in life history. *Oikos*, 126:472–479, 2017.

E. Bouin, V. Calvez, N. Meunier, S. Mirrahimi, B. Perthame, G. Raoul, and R. Voituriez. Invasion fronts with variable motility: Phenotype selection, spatial sorting and wave acceleration. *Comptes Rendus Mathematique*, 350:761–766, 2012.

O. J. Burton, B. L. Phillips, and J. M. J. Travis. Trade-offs and the evolution of life-histories during range expansion. *Ecology Letters*, 13:1210–1220, 2010.

P.-O. Cheptou, O. Carrue, S. Rouifed, and A. Cantarel. Rapid evolution of seed dispersal in an urban environment in the weed crepis sancta. *Proceedings of the National Academy of Sciences*, 105:3796–3799, 2008.

J. S. Clark, C. Fastie, G. Hurtt, S. T. Jackson, C. Johnson, G. A. King, M. Lewis, J. Lynch, S. Pacala, C. Prentice, E. W. Schupp, T. Webb, and P. Wyckoff. Reid's paradox of rapid plant migration - dispersal theory and interpretation of paleoecological records. *Bioscience*, 48:13–24, 1998a.

J.S. Clark. Why trees migrate so fast: Confronting theory with dispersal biology and the paleorecord. *The Americal Naturalist*, 152:204–224, 1998.

J.S. Clark, E. Macklin, and L. Wood. Stages and spatial scales of recruitment limitation in southern appalachian forests. *Ecological Monographs*, 68:213–235, 1998b.

J. Cote, E. Bestion, S. Jacob, J. Travis, D. Legrand, and M. Baguette. Evolution of dispersal strategies and dispersal syndromes in fragmented landscapes. *Ecography*, 40:56–73, 2017.

L. C. Cwynar and G. M. MacDonald. Geographical variation of lodgepole pine in relation to population history. *The Americal Naturalist*, 129:463–469, 1987.

E.C. Elliott and S.J. Cornell. Dispersal polymorphism and the speed of biological invasions. *PloS one*, page e40496, 2012.

S. P. Ellner. Rapid evolution: from genes to communities, and back again? *Functional Ecology*, 27:1087–1099, 2013.

S.P. Ellner and S.J. Schreiber. Temporally variable dispersal and demography can accelerate the spread of invading species. *Theoretical Population Biology*, 82:283–298, 2012.

R. A. Fisher. The wave of advance of advantageous genes. *Annals of Eugenics*, 7:355–369, 1937.

A. Hastings, K. Cuddington, K. F. Davies, C. J. Dugaw, S. Elmendorf, A. Freestone, S. Harrison, M. Holland, J. Lambrinos, U. Malvadkar, B. A. Melbourne, K. Moore, C. Taylor, and D. Thomson. The spatial spread of invasions: new developments in theory and evidence. *Ecology Letters*, 8:91–101, 2005.

A.A. Hoffmann and C.M. Sgro. Climate change and evolutionary adaptation. *Nature*, 470: 479, 2011.

F. Huang, S. Peng, B. Chen, H. Liao, Q. Huang, Z. Lin, and G. Liu. Rapid evolution of dispersal-related traits during range expansion of an invasive vine *Mikania micrantha*. *Oikos*, 124:1023–1030, 2015.

C.L. Hughes, C. Dytham, and J.K. Hill. Modelling and analysing evolution of dispersal in populations at expanding range boundaries. *Ecological Entomology*, 32:437–445, 2007.

S. K. Jindal, D. Arora, and T. R. Ghai. Variability studies for yield and its contributing traits in okra. *Electronic Journal of Plant Breeding*, 1:1495–1499, 2010.

J. S. Johnson, R. S. Cantrell, C. Cosner, F. Hartig, A. Hastings, H. S. Rogers, E. W. Schupp, K. Shea, B. J. Teller, X. Yu, D. Zurell, and G. Pufal. Rapid changes in seed dispersal traits may modify plant responses to global change. *AoB Plants*, page plz020, 2019.

E. Jongejans, O. Skarpaas, and K. Shea. Dispersal, demography and spatial population models for conservation and control management. *Perspectives in Plant Ecology Evolution and Systematics*, 9:153–170, 2008.

E. Jongejans, K. Shea, O. Skarpaas, D. Kelly, and S. P. Ellner. Importance of individual and environmental variation for invasive species spread: a spatial integral projection model. *Ecology*, 92:86–97, 2011.

M. Kot, M. A. Lewis, and P. van den Driessche. Dispersal data and the spread of invading organisms. *Ecology*, 77:2027–2042, 1996.

U. Liberman and M.W. Feldman. Modifiers of mutation rate: a general reduction principle. *Theoretical Population Biology*, 30:125–142, 1986.

J.O. Lloyd-Smith, S.J. Schreiber, P.E. Kopp, and W.M. Getz. Superspreading and the effect of individual variation on disease emergence. *Nature*, 438:355–9, 2005.

E. V. Moran, F. Hartig, and D. M. Bell. Intraspecific trait variation across scales: implications for understanding global change responses. *Global Change Biology*, 22:137–150, 2016.

M.G. Neubert and H. Caswell. Demography and dispersal: Calculation and sensitivity analysis of invasion speed for structured populations. *Ecology*, 81:1613–1628, 2000.

J. M. Norghauer and D. M. Newbery. Tree size and fecundity influence ballistic seed dispersal of two dominant mast-fruiting species in a tropical rain forest. *Forest Ecology and Management*, 338:100–113, 2015.

J. M. Norghauer, C. A. Nock, and J. Grogan. The importance of tree size and fecundity for wind dispersal of big-leaf mahogany. *PloS One*, 6:e17488, 2011.

H.M. Pereira, P.W. Leadley, V. Proença, R. Alkemade, J. P. W. Scharlemann, J. F. Fernandez-Manjarrés, M. B. Araújo, P. Balvanera, R. Biggs, W. W. L. Cheung, L. Chini, H. D. Cooper, E. L. Gilman, S. Guénette, G. C. Hurtt, H. P. Huntington, G. M. Mace, T. Oberdorff, C. Revenga, P. Rodrigues, R. J. Scholes, U. R. Sumaila, and M. Walpole. Scenarios for global biodiversity in the 21st century. *Science*, 330:1496–1501, 2010.

T. A. Perkins, B. L. Phillips, M. L. Baskett, and A. Hastings. Evolution of dispersal and life history interact to drive accelerating spread of an invasive species. *Ecology Letters*, 16: 1079–1087, 2013.

S. Petrovskii and A. Morozov. Dispersal in a statistically structured population: fat tails revisited. *The American Naturalist*, 173:278–289, 2008.

B. L. Phillips, G. P. Brown, and R. Shine. Life-history evolution in range-shifting populations. *Ecology*, 91:1617–1627, 2010.

B.L. Phillips, G.P. Brown, J.M.J. Travis, and R. Shine. Reid's paradox revisited: the evolution of dispersal kernels during range expansion. *American Naturalist*, 172:S34–S48, 2008.

T.C. Reluga. The importance of being atomic: Ecological invasions as random walks instead of waves. *Theoretical Population Biology*, 112:157–169, 2016.

Ophelie Ronce and Jean Clobert. *Dispersal Syndromes*, book section 10, pages 119–138. Oxford University of Press, United Kingdom, 2012.

M. Saastamoinen, G. Bocedi, J. Cote, D. Legrand, F. Guillaume, C. W. Wheat, E.A. Fronhofer, C. Garcia, R. Henry, A. Husby, M. Baguette, D. Bonte, A. Coulon, H. Kokko, E. Matthysen, K. Niitepõld, E. Nonaka, V. M. Stevens, J. M. J. Travis, K. Donohue, J. M. Bullock, and M. del Mar Delgado. Genetics of dispersal. *Biological Reviews*, 93:574–599, 2018.

L. Santini, T. Cornulier, J.M. Bullock, S.C.F. Palmer, S.M. White, G. Bocedi, C. Rondinini, and J.M.J. Travis. Modelling spread rate in terrestrial mammals and the ability to track a shifting climate: a trait space approach. *Global Change Biology*, 22:2415–2424, 2016.

E. W. Schupp, R. Zwolak, Jones L. R, R. S. Snell, N. G. Beckman, C. Aslan, B. R. Cavazos, E. Effiom, E. C. Fricke, F. Montaño-Centellas, J. Poulsen, O. H. Razafindratsima, M. E. Sandor, and K. Shea. Intrinsic and extrinsic drivers of intraspecific variation in seed dispersal are diverse and pervasive. *AoB Plants*, in revision.

K. Shea, E. Jongejans, O. Skarpaas, D. Kelly, and A. W. Sheppard. Optimal management strategies to control local population growth or population spread may not be the same. *Ecological Applications*, 20:1148–1161, 2010.

J. G. Skellam. Random dispersal in theoretical populations. *Biometrika*, 38:196–218, 1951.

R.S. Snell, N.G. Beckman, E. Fricke, B.A. Loiselle, C.S. Carvalho, L.R. Jones, N.I. Lichti, N. Lustenhouwer, S. Schreiber, C. Strickland, L.L. Sullivan, B.R. Cavazos, I. Giladi, A. Hastings, K. Holbrook, E. Jongejans, O. Kogan, F. Montaño-Centellas, J. Rudolph, H. S Rogers, R. Zwolak, and E. Schupp. Consequences of intraspecific variation in seed dispersal for plant demography, communities, evolution, and global change. *AoB PLANTS*, 03 2019.

R.E. Snyder. How demographic stochasticity can slow biological invasions. *Ecology*, pages 1333–1339, 2003.

J.P. Stover, B.E. Kendall, and R.M. Nisbet. Consequences of dispersal heterogeneity for population spread and persistence. *Bulletin of Mathematical Biology*, 76:2681–2710, 2014.

S. Tabassum and M. R. Leishman. Have your cake and eat it too: greater dispersal ability and faster germination towards range edges of an invasive plant species in eastern australia. *Biological Invasions*, 20:1199–1210, 2018.

S. Tabassum and M. R. Leishman. It doesn't take two to tango: increased capacity for self-fertilization towards range edges of two coastal invasive plant species in eastern australia. *Biological Invasions*, 21:1–13, 2019.

M.W. Tingley, W.B. Monahan, S.R. Beissinger, and C. Moritz. Birds track their grinnellian niche through a century of climate change. *Proceedings of the National Academy of Sciences*, 106:19637–19643, 2009.

J. M. J. Travis and C. Dytham. Dispersal evolution during invasions. *Evolutionary Ecology Research*, 4:1119–1129, 2002.

J. M. J. Travis, K. Mustin, T. G. Benton, and C. Dytham. Accelerating invasion rates result from the evolution of density-dependent dispersal. *Journal of Theoretical Biology*, 259: 151–158, 2009.

J. M. J. Travis, Catriona M. Harris, K. J. Park, and J. M. Bullock. Improving prediction and management of range expansions by combining analytical and individual-based modelling approaches. *Methods in Ecology and Evolution*, 2:477–488, 2011.

M. C. Urban, G. Bocedi, A. P. Hendry, J.-B. Mihoub, G. Pe'er, A. Singer, J. R. Bridle, L. G. Crozier, L. De Meester, W. Godsoe, A. Gonzalez, J. J. Hellmann, R. D. Holt, A. Huth, K. Johst, C. B. Krug, P. W. Leadley, S. C. F. Palmer, J. H. Pantel, A. Schmitz, P. A. Zollner, and J. M. J. Travis. Improving the forecast for biodiversity under climate change. *Science*, 353, 2016.

M. G. Usman, M. Y. Rafii, M. R. Ismail, M. A. Malek, and M. Abdul Latif. Heritability and genetic advance among chili pepper genotypes for heat tolerance and morphophysiological characteristics. *The Scientific World Journal*, 2014:14, 2014.

J. L. Williams, B. E. Kendall, and J. M. Levine. Rapid evolution accelerates plant population spread in fragmented experimental landscapes. *Science*, 353:482–485, 2016a.

J. L. Williams, R. E. Snyder, and J. M. Levine. The influence of evolution on population spread through patchy landscapes. *American Naturalist*, 188:15–26, 2016b.

Appendix A: Derivations for the random transmission model

In this Appendix derivations of the main analytic results are presented. As in the main text, let F and L be random variables with joint density function $\rho(f,\ell)$. Then we can rewrite (1) as

$$n_{t+1}(x) = \int_{-\infty}^{\infty} \mathbb{E}\left[k_L(x-y)F\right] D(n_t(y))n_t(y)dy \tag{9}$$

and $\lambda(s)$ from the methods section in the main text can be rewritten as

$$\lambda(s) = \int_{-\infty}^{\infty} \mathbb{E}[Fk_1(v/L)/L]\exp(-sv)dv.$$

Provided that F and L have a finite variances, we can always write $F = \overline{F} + \sigma_F Z_F$ and $L = \overline{L} + \sigma_L Z_L$ where Z_F, Z_L are random variables with mean zero and variance 1, $\overline{F}$ and $\overline{L}$ are the expected values of F and L, and σ_F^2 and σ_L^2 are the variances of F and L. Let r denote the correlation between F and L.

To derive the small variance approximations, we assume that there are positive constants τ_F, τ_L such that $\sigma_F = \varepsilon\tau_F$ and $\sigma_L = \varepsilon\tau_L$ for small $\varepsilon > 0$. Ellner and Schreiber [2012] showed that

$$\frac{d^k c^*}{d\varepsilon^k}\Big|_{\varepsilon=0} = \frac{1}{s^*}\frac{\partial^k \log\lambda}{\partial\varepsilon^k}\Big|_{\varepsilon=0}(s^*) \tag{10}$$

where s^* is such that $c^* = \lambda(s^*)/s^*$ for $\varepsilon = 0$. By Tonelli's theorem,

$$\lambda(s) = \int_{-\infty}^{\infty} \mathbb{E}[Fk_1(v/L)/L]\exp(-sv)dv = \mathbb{E}\left[\int_{-\infty}^{\infty} Fk_1(v/L)/L\exp(-sv)dv\right] = \mathbb{E}[FM(Ls)]$$

where $M(s) = \int_{-\infty}^{\infty} k_1(v)\exp(-sv)dv$. Differentiating with respect to ε and evaluating at zero yields

$$\begin{aligned}\frac{\partial\lambda}{\partial\varepsilon}\Big|_{\varepsilon=0} =& \frac{\partial}{\partial\varepsilon}\Big|_{\varepsilon=0}\mathbb{E}[\left(\overline{F}+\varepsilon\tau_F Z_F\right) M\left((\overline{L}+\varepsilon\tau_L Z_L)s\right)]\\ =&\mathbb{E}[\tau_F Z_F M\left((\overline{L}+\varepsilon\tau_L Z_L)s\right) + \left(\overline{F}+\varepsilon\tau_F Z_F\right) M'\left((\overline{L}+\varepsilon\tau_L Z_L)s\right)\tau_L Z_L s]\Big|_{\varepsilon=0}\\ =&\mathbb{E}[\tau_F Z_F M\left(\overline{L}s\right) + \overline{F}M'\left(\overline{L}s\right)\tau_L Z_L s] = 0.\end{aligned}$$

Hence, we get

$$\frac{\partial\log\lambda}{\partial\varepsilon}\Big|_{\varepsilon=0} = \frac{1}{\lambda}\frac{\partial\lambda}{\partial\varepsilon}\Big|_{\varepsilon=0} = 0. \tag{11}$$

Differentiating a second time with respect to ε and evaluating at zero yields

$$\frac{\partial^2\log\lambda}{\partial\varepsilon^2}\Big|_{\varepsilon=0} = -\frac{1}{\lambda^2}\left(\frac{\partial\lambda}{\partial\varepsilon}\right)^2\Big|_{\varepsilon=0} + \frac{1}{\lambda}\frac{\partial^2\lambda}{\partial\varepsilon^2}\Big|_{\varepsilon=0} = \frac{1}{\lambda}\frac{\partial^2\lambda}{\partial\varepsilon^2}\Big|_{\varepsilon=0}. \tag{12}$$

Computing the second derivative of λ yields

(13)
$$\begin{aligned}\frac{\partial^2\lambda}{\partial\varepsilon^2}\Big|_{\varepsilon=0} =&\frac{\partial^2}{\partial\varepsilon^2}\Big|_{\varepsilon=0}\mathbb{E}[\left(\overline{F}+\varepsilon\tau_F Z_F\right) M\left((\overline{L}+\varepsilon\tau_L Z_L)s\right)]\\ =&\frac{\partial}{\partial\varepsilon}\Big|_{\varepsilon=0}\mathbb{E}[\tau_F Z_F M\left((\overline{L}+\varepsilon\tau_L Z_L)s\right)+\left(\overline{F}+\varepsilon\tau_F Z_F\right) M'\left((\overline{L}+\varepsilon\tau_L Z_L)s\right)\tau_L Z_L s]\\ =&\mathbb{E}[2\tau_F Z_F M_1\tau_L Z_L s+\overline{F}M_2(\tau_L Z_L s^*)^2]\\ =&2M_1\tau_F\tau_L r\, s+\overline{F}M_2\tau_L^2(s^*)^2\end{aligned}$$

where $M_1 = M'(\overline{L}s^*)$ and $M_2 = M''(\overline{L}s^*)$. Recalling that $\sigma_F = \varepsilon\tau_F$, $\sigma_L = \varepsilon\tau_L$ and $\lambda|_{\varepsilon=0} = \overline{F}M_0$ where $M_0 = M(\overline{L}s^*)$, equations (10)–(13) give the second order approximation

$$\begin{aligned}c^*(\varepsilon) =&c^*(0)+\frac{\varepsilon^2}{2\overline{F}M_0 s^*}\left(2M_1\tau_F\tau_L r\, s^*+\overline{F}M_2\tau_L^2(s^*)^2\right)+O(\varepsilon^3)\\ =&c^*(0)+\frac{M_1}{\overline{F}M_0}\sigma_F\sigma_L r+\frac{M_2 s^*}{2M_0}\sigma_L^2+O(\varepsilon^3).\end{aligned} \tag{14}$$

Defining $m(s) = \int_{-\infty}^{\infty} k_1(v/\overline{L})/\overline{L}e^{vs}ds = M(\overline{L}s)$, we get $m'(s) = M'(\overline{L}s)\overline{L}$ and $m''(s) = M''(\overline{L}s)\overline{L}^2$. Hence, $M_0 = m(s^*)$, $M_1 = m'(s^*)/\overline{L}$ and $M_2 = m''(s^*)/\overline{L}^2$ and

$$c^*(\varepsilon) = c^*(0)+\frac{m'(s^*)}{m(s^*)}\frac{\sigma_F}{\overline{F}}\frac{\sigma_L}{\overline{L}}r+\frac{m''(s^*)s^*}{2m(s^*)}\left(\frac{\sigma_L}{\overline{L}}\right)^2+O(\varepsilon^3) \tag{15}$$

which gives equations (4) and (7) from the main text.

Appendix B: Derivation of the perfect transmission approximations

For the model with perfect transmission, recall that we have the demographic-dispersal kernel $K_\nu(f,\ell;f',\ell,v)$ (now parameterized by ν) given by

$$K_\nu(f,\ell;f',\ell',v) = k_\ell(v)f\left(\nu\delta_{(f,\ell)}(f',\ell')+(1-\nu)\rho(f',\ell')\right) \tag{16}$$

where $\delta_{(f,\ell)}(f',\ell')$ is the Dirac delta function based at the point (f,ℓ). Let $H_\nu(s)$ be the operator that takes the function $n(f,\ell)$ to the function

$$(H_\nu(s)n)(f',\ell') = \int_{-\infty}^{\infty}\left(\iint K_\nu(f,\ell;f',\ell',v)e^{sv}n(f,\ell)df\,d\ell\right)dv \tag{17}$$

and let $\lambda_\nu(s)$ be the dominant eigenvalue of $H(s)$. The rate of spatial spread, as a function of ν, is given by $c_\nu^* = \min_{s>0}\lambda_\nu(s)/s$. Let s^* be the value of s that gives the rate of spread for $\nu = 0$ i.e. only random transmission.

Ellner and Schreiber [2012] showed that

$$\frac{dc_\nu^*}{d\nu}\Big|_{\nu=0} = \frac{1}{s^*}\frac{\partial\log\lambda_\nu}{\partial\nu}\Big|_{\nu=0}(s^*) = \frac{1}{\lambda_0\, s^*}\frac{\partial\lambda_\nu}{\partial\nu}\Big|_{\nu=0}(s^*). \tag{18}$$

To find this derivative, we need to find the dominant, left and right eigenfunctions of $H_0(s^*)$. The dominant, right eigenfunction w and eigenvalue λ_0 must satisfy

$$\begin{aligned}\lambda_0 w(f',\ell') &= \int_{-\infty}^{\infty}\iint k_\ell(v) f\rho(f,\ell;f',\ell')w(f,\ell)e^{s^*v}df d\ell dv\\ &= \iint\left(\int_{-\infty}^{\infty} k_\ell(v)e^{s^*v}dv\right) f\rho(f',\ell')w(f,\ell)df d\ell\\ &= \iint M(\ell s^*) f\rho(f',\ell')w(f,\ell)df d\ell\\ &= \rho(f',\ell')\iint M(\ell s^*) f w(f,\ell)df d\ell\end{aligned}$$

Hence, we get the unique, normalized eigenfunction is $w(f,\ell)=\rho(f,\ell)$ and eigenvalue is $\lambda_0=\iint M(\ell s^*)f\rho(f,\ell)df d\ell = \mathbb{E}[FM(Ls^*)]$ where (F,L) is the random vector with density function $\rho(f,\ell)$. The dominant, left eigenfunction $u(f,\ell)$ must satisfy

$$\lambda_0 u(f,\ell) = fM(\ell s^*)\iint u(f',\ell')\rho(f',\ell')df' d\ell'$$

and therefore can be chosen to equal $u(f,\ell)=fM(\ell s^*)$. Hence, we get

$$\frac{\partial\lambda_\nu}{\partial\nu}\Big|_{\nu=0}(s^*) = \frac{\iint u(f,\ell)(Gw)(f,\ell)df d\ell}{\iint u(f,\ell)w(f,\ell)df d\ell}$$

where G is the perturbation operator on functions $n(f,\ell)$ defined by

$$(Gn)(f',\ell') = \int_{-\infty}^{\infty}\iint f\left(\delta_{f',\ell'}(f,\ell)-\rho(f',\ell')\right)n(f,\ell)e^{-s^*v}k_\ell(v)df d\ell dv.$$

We have $\iint u(f,\ell)w(f,\ell)df d\ell = \iint fM(\ell s^*)\rho(\ell,f)d\ell df = \mathbb{E}[FM(Ls^*)]=\lambda_0$. Furthermore,

$$\begin{aligned}\iint u(f,\ell)(Gw)(f,\ell)df d\ell &= \iint u(f,\ell)\left(fM(\ell s^*)\rho(f,\ell)-\rho(f,\ell)\lambda_0\right)df d\ell\\ &= \iint fM(\ell s^*)\left(fM(\ell s^*)\rho(f,\ell)-\rho(f,\ell)\mathbb{E}[FM(Ls^*)]\right)df d\ell\\ &= \iint (fM(\ell s^*))^2\rho(f,\ell)df d\ell - \mathbb{E}[FM(Ls^*)]^2\\ &= \mathbb{E}[(FM(Ls^*))^2]-\mathbb{E}[FM(Ls^*)]^2 = \mathrm{Var[FM(Ls^*)]}.\end{aligned}$$

Thus, we get

$$\frac{dc_\nu^*}{d\nu}\Big|_{\nu=0} = \frac{1}{\lambda_0 s^*}\frac{\mathrm{Var[FM(Ls^*)]}}{\mathbb{E}[FM(Ls^*)]} \tag{19}$$

As in Appendix A, let $F=\overline{F}+\sigma_F Z_F$ and $L=\overline{L}+\sigma_L Z_L$ where Z_F, Z_L are random variables with mean zero and variance 1, $\overline{F}$ and $\overline{L}$ are the expected values of F and L, and σ_F^2 and σ_L^2 are the variances of F and L. Let r denote the correlation between F and L. To derive the small variance approximations, we assume that there are positive constants τ_F,τ_L such that $\sigma_F=\varepsilon\tau_F$ and $\sigma_L=\varepsilon\tau_L$ for small $\varepsilon>0$. With these assumptions, to get an

approximation of Var[FM(Ls*)] for small ε, we need the following three approximations

$$\begin{aligned}\mathbb{E}[FM(Ls^*)] =&\mathbb{E}\left[(\overline{F}+\sigma_F Z_F)(M_0+M_1\sigma_L Z_L s^*+M_2(\sigma_L Z_L s^*)^2/2)\right]+O(\varepsilon^3)\\ =&\overline{F}(M_0+M_2(\sigma_L s^*)^2/2)+M_1\sigma_F\sigma_L r s^*+O(\varepsilon^3)\end{aligned} \tag{20}$$

where $M_0 = M(\overline{L}s^*)$, $M_1 = M'(\overline{L}s^*)$ and $M_2 = M''(\overline{L}s^*)$, and

$$\mathbb{E}[FM(Ls^*)]^2 =(\overline{F}M_0)^2+\overline{F}^2M_0M_2(\sigma_L s^*)^2+2\overline{F}M_0M_1\sigma_F\sigma_L r s^*+O(\varepsilon^3), \tag{21}$$

and

$$\begin{aligned}\mathbb{E}[(FM(Ls^*))^2] =&\mathbb{E}\left[\left((\overline{F}+\sigma_F Z_F)(M_0+M_1\sigma_L Z_L s^*+M_2(\sigma_L Z_L s^*)^2/2\right)^2\right]\\ &+O(\varepsilon^3)\\ =&\mathbb{E}\left[\left(\overline{F}M_0+\overline{F}M_1\sigma_L Z_L s^*+\overline{F}M_2(\sigma_L Z_L s^*)^2/2+\sigma_F Z_F M_0+\sigma_F Z_F M_1\sigma_L Z_L s^*\right)^2\right]\\ &+O(\varepsilon^3)\\ =&(\overline{F}M_0)^2+\overline{F}M_0\overline{F}M_2(\sigma_L s^*)^2+2\overline{F}M_0M_1\sigma_L\sigma_F r s^*+(\overline{F}M_1\sigma_L s^*)^2\\ &+2\overline{F}M_0M_1\sigma_L\sigma_F r s^*+M_0^2\sigma_F^2+O(\varepsilon^3).\end{aligned} \tag{22}$$

Taking the difference between (22) and (21) gives us

$$\mathrm{Var[FM(Ls^*)]} =(\overline{F}M_1\sigma_L s^*)^2+2\overline{F}M_0M_1\sigma_L\sigma_F r s^*+M_0^2\sigma_F^2+O(\varepsilon^3). \tag{23}$$

Thus, for sufficiently small ν and ε, equation (19) and $\lambda_0 = \overline{F}M_0$ implies that

$$\begin{aligned}c_\nu^* \approx& c^*+\frac{\nu}{\overline{F}M_0 s^*}\frac{(\overline{F}M_1\sigma_L s^*)^2+2\overline{F}M_0M_1\sigma_L\sigma_F r s^*+M_0^2\sigma_F^2}{\overline{F}M_0}\\ =&c^*+\nu\left(\frac{M_1^2 s^*}{M_0^2}\sigma_L^2+\frac{2M_1}{\overline{F}M_0}\sigma_L\sigma_F r+\frac{1}{\overline{F}^2 s^*}\sigma_F^2\right).\end{aligned} \tag{24}$$

Defining $m(s) = \int_{-\infty}^{\infty} k_1(v/\overline{L})/\overline{L}e^{vs}ds = M(\overline{L}s)$, we get $m'(s) = M'(\overline{L}s)\overline{L}$ and $m''(s) = M''(\overline{L}s)\overline{L}^2$. Hence, $M_0 = m(s^*)$, $M_1 = m'(s^*)/\overline{L}$ and $M_2 = m''(s^*)/\overline{L}^2$ and

$$c_\nu^* \approx c^*+\nu\left(\frac{m_1(s^*)^2 s^*}{m(s^*)^2}\frac{\sigma_L^2}{\overline{L}^2}+\frac{2m_1(s^*)}{m(s^*)}\frac{\sigma_L}{\overline{L}}\frac{\sigma_F}{\overline{F}}r+\frac{1}{s^*}\left(\frac{\sigma_F}{\overline{F}}\right)^2\right) \tag{25}$$

which gives equations (5), (6), and (8) from the main text.

Department of Evolution and Ecology and Center for Population Biology, University of California, Davis, California USA 95616

Department of Biology and Ecology Center, Utah State University, Logan, Utah 84322